9-2000

Modeling of Conductive Transport in Proton-Exchange Membranes for Fuel Cells

T. Thampan

S. Malhotra

H. Tang

Ravindra Datta
Worcester Polytechnic Institute, rdatta@wpi.edu

Journal of The Electrochemical Society, **147** (9) 3242-3250 (2000)
S0013-4651(00)01-112-5 CCC: $7.00

Modeling of Conductive Transport in Proton-Exchange Membranes for Fuel Cells

Tony Thampan,[a] Sanjiv Malhotra,[b,*] Hao Tang,[a,b] and Ravindra Datta[a,*,z]

[a]*Department of Chemical Engineering, Worcester Polytechnic Institute, Worcester, Massachusetts 01609, USA*
[b]*H Power Corporation, Belleville, New Jersey 07179, USA*
[c]*PlugPower, Latham, New York 12110, USA*

An adequate understanding of the conductivity of polyperfluorosulfonic acid (PFSA) membranes as a function of water content, or relative humidity, and temperature is necessary for an analysis of the functioning of proton-exchange membrane (PEM) fuel cells. Although much work has been done toward elucidating the microstructure and conduction mechanism in PFSA, a satisfactory theoretical model with a minimum of fitted parameters is not yet available. Such a model is developed here for the conduction of protons in hydrated Nafion® or like membranes based on the dusty-fluid model for transport and the percolation model for structural aspects. Further, thermodynamics of dissociation of the acid groups in the presence of polar solvents such as water is included. The sorption of solvent from vapor is modeled using a finite-layer Brunauer-Emmett-Teller (BET) model. With the only fitted parameters employed being the BET constants, determined independently, and the ratio of diffusion coefficients representing the interaction of the protonated solvent molecules with solvent and that with the membrane, the model provides excellent correlation with a variety of experimental data.

Manuscript submitted January 26, 2000; revised manuscript received May 26, 2000.

The proton-exchange membrane (PEM) fuel cell has lately emerged as a highly promising power source for a wide range of applications. The solid polymer electrolyte utilized in these fuel cells is typically a polyperfluorosulfonic acid (PFSA) membrane (*e.g.*, Nafion®, manufactured by DuPont), that provides excellent performance in the presence of water by virtue of its strong acidity, low permeability of hydrogen and oxygen, and good electrochemical stability in the presence of electrocatalysts. This has allowed the development of low-temperature PEM fuel cells with impressive current densities. These membranes have also been widely utilized in the chlor-alkali industry. However, an understanding and modeling of the transport of ionic species through these ion-exchange membranes is not yet adequately developed, especially for proton transport, which is the focus of this paper.

There are numerous studies on the nanostructural aspects of the Nafion membranes.[1-15] The unique properties of these PFSA membranes are attributable to their polymer structure that consists of a fluorocarbon, Teflon-like, backbone with side chains terminating in $-SO_3H$ groups. In the presence of water or other polar solvents, these sulfonic acid groups dissociate, protonating the solvent molecules and forming a hydrophilic phase that also includes the solvated $-SO_3^-$ ions tethered to the hydrophobic backbone through the side chains.[1] Based on small angle X-ray and other studies,[2-4] Gierke and co-workers[2,15] proposed in their "cluster–network model" that the incompatibility of the fluorocarbon and the ionic/solvent component leads to the formation of inverted micelles, existing as near-spherical aggregates, 3 to 5 nm in diameter, depending upon the level of hydration. These are interconnected through short narrow channels, 1 to 2 nm in diameter, to provide a network for diffusion interspersed throughout the fluorocarbon matrix. The extent of the solvent uptake and membrane swelling is controlled by a balance between the internal osmotic pressure of solvent in the pores and the elastic forces of the polymer matrix,[16] which, in turn, depend upon the temperature and membrane pretreatment. The cluster–network model provides a suitable structural framework for the development of ionic transport models in these membranes akin to those in porous media, *e.g.*, the parallel-pore model or the percolation model.

There is, of course, substantial literature on the modeling of transport through ion-exchange membranes,[17–20] although the majority of the work deals with the transport of electrolytes, *i.e.*, salt/acid/base solutions, rather than with proton transport. The interest in diffusion of electrolytes through ion-exchange membranes stems mainly from their chlor-alkali and electrodialysis applications. A theoretical model of ion-exchange membranes involves (*i*) a structural model and (*ii*) a transport model. The cluster-network, the parallel-pore, and the percolation models referred to above belong to the former. As to the latter, there are three alternate approaches: (*i*) phenomenological models based on nonequilibrium thermodynamics,[21,22] (*ii*) models based on the Nernst-Planck equations,[19,23,24] and (*iii*) those based on the generalized Stefan-Maxwell (GSM) equations,[25-27] or equivalently, the frictional formalism of Spiegler.[20,28] The last two are of a similar form, the former involving diffusion coefficients and the latter incorporating frictional coefficients. The transport model of choice is suitably adapted to the chosen structural model to provide an overall description of ion transport in a membrane.

Fairly sophisticated capillary-pore models incorporating the Nernst-Planck equations to describe diffusion, the Navier-Stokes equations for convective flow, and the Poisson-Boltzmann equation to describe the radial potential profile within individual pores have been developed,[23,24,29,30] that adequately simulate the transport of alkali metal ions through the membrane. However, the GSM equations, or equivalently Spiegler's frictional model, represent a more general starting point, the Nernst-Planck equations being strictly applicable to dilute solutions.[31] The GSM equations have been utilized with a fair degree of success by Spiegler,[28] Meares *et al.*,[20] Pintauro and Bennion,[27] Wesselingh *et al.*,[32] and van der Stegen *et al.*,[33] for describing the transport of alkali electrolytes in ion-exchange membranes. The main limitation, however, is that many of the necessary GSM diffusion coefficients are not independently available in the literature, requiring their treatment as fitted parameters.[33]

The status of the modeling of transport of protons in hydrated PFSA membranes is less satisfactory, although there is much of relevance in the electrolyte transport literature. A number of experimental studies have, however, been performed under a variety of conditions.[10,15-18] These conductivity data show that at very low water uptake, *i.e.*, for number of water molecules per $-SO_3H$ group, $\lambda < 2$, the Nafion membrane behaves essentially as an insulator, the conductivity σ being of the order of 10^{-7} S/cm.[34] Beyond a critical hydration level uptake ($\lambda \approx 2$), or a "percolation" threshold, σ rises dramatically with water uptake reaching a plateau in the semiconductor range, of the order of about 10^{-1} S/cm, for a membrane immersed in water. In general, σ also rises with temperature, although the data of Sone *et al.*[35] indicate a low-temperature range with

* Electrochemical Society Active Member.
z E-mail: rdatta@wpi.edu

S0013-4651(00)01-112-5 CCC: $7.00

anamolous behavior. Since the water uptake is determined by relative humidity (RH), temperature, and membrane pretreatment, these are the key factors affecting membrane conductivity.

Fadley and Wallace[36] developed an absolute-rate model for conduction in PEMs, in which the effect of hydration was included by assuming that it affected the Gibbs free energy of activation. The model agreed with data in the range of $0 < \lambda < 5$, but not beyond that. Hsu *et al.*[10] developed a percolation model to describe the effect of water uptake on conductivity, *i.e.*, $\sigma = \sigma_0 (\epsilon - \epsilon_0)^q$. The expression fitted the data well with the following parameters $q = 1.5$, $\sigma_0 = 0.16$ S/cm, and $\epsilon_0 = 0.1$. No attempt, however, was made to predict σ_0 in terms of more fundamental transport parameters. Morris and Sun[37] also found the percolation model to be accurate but with different fitted parameters, namely, $q = 1.95$, $\sigma_0 = 0.125$ S/cm, and $\epsilon_0 = 0.06$. Springer *et al.*[38] developed an empirical model to relate the conductivity linearly to λ, instead of to ϵ, and used the Arrhenius equation to describe temperature dependence of conductivity. In turn, λ was fitted to RH through a third-order polynomial. Eikerling *et al.*[39] extended the percolation model by considering two different types of pores, those with only surface water and others containing additional bulk-like water, and ascribed different conductivities to each. Then by connecting the pores randomly within the framework of the random-network theory, they predicted conductivity as a function of hydration level. Bernardi and Verbrugge[40] utilized the Nernst-Planck equation along with a parallel-pore model to describe membrane conductivity within a larger model to predict PEM fuel-cell performance. However, a direct comparison of the model with conductivity data was not provided. More recently, there have been attempts to do molecular simulation of proton transport within pores of Nafion.[41,42]

The model developed here is based on the assumption that the diffusion mechanism in hydrated PEMs is similar to that in the liquid, *i.e.*, protons are transported as hydronium ions via mutual diffusion, Grotthus mechanism, and flow through pores containing water within the ionomer,[34] rather than, *e.g.*, through surface site-hopping. The hydronium ions in the liquid phase result from dissociation of the acid groups. The obstruction presented by the polymer matrix to the diffusion of hydronium ions is modeled as an additional frictional, or diffusional, interaction with the large "dust" particles (Fig. 1), representing the polymer species in the spirit of the "dusty-fluid model" (DFM),[43] with a molecular weight equal to the polymer equivalent weight (EW). The space filling aspects and tortuosity of the polymer matrix are accounted for through the DFM structural constants, which also include provision for the absence of conduction below a percolation threshold. Thermodynamics of sulfonic acid group solvation and the water sorption isotherm are included as well, as is the swelling of the membrane. Since it has been the subject of considerable study,[44] the model is utilized for hydrated Nafion. However, it should be applicable to other PEMs as well as to solvents other than water.

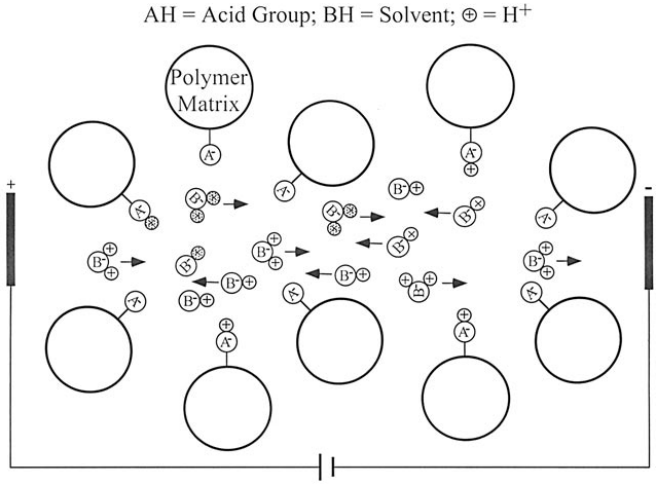

Figure 1. A "dusty-fluid model" depiction of a PEM. The polymer matrix along with an acid groups is viewed as "dust" particles comprising the PEM. The membrane imbibes a polar solvent BH (*e.g.*, HOH, CH_3OH), that solvates the protons from the pendant acid HA forming BH_2^+ that serves as the charge carrier.

Theory

General transport model for ion-exchange membranes.—We start with the generalized Stefan-Maxwell equations with the electrochemical potential gradient as the driving force for describing the diffusional velocity of species *i*, $\boldsymbol{\nu}_i^D$, in a continuum fluid[26,31]

$$\frac{-c_i}{RT}\nabla_T\mu_i^e = \sum_{\substack{j=1\\ j\neq i}}^{n}\frac{c_i c_j}{cD_{ij}}(\boldsymbol{\nu}_i^D - \boldsymbol{\nu}_j^D) \qquad (i = 1, 2, ..., n) \qquad [1]$$

In Eq. 1, the electrochemical potential gradient at constant temperature is composed of chemical and electrical potential gradients

$$\nabla_T\mu_i^e = \nabla_T\mu_i + z_iF\nabla\Phi = (RT\nabla\ln c_i + RT\nabla\ln\gamma_i + \bar{V}_i\nabla p) + z_iF\nabla\Phi \qquad [2]$$

Equation 1 may alternatively be written as per the frictional formalism of Spiegler[28]

$$-c_i\nabla_T\mu_i^e = \sum_{\substack{j=1\\ j\neq i}}^{n} c_i c_j\zeta_{ij}(\boldsymbol{\nu}_i^D - \boldsymbol{\nu}_j^D) \qquad (i = 1, 2, ..., n) \qquad [3]$$

where the frictional coefficients and the diffusion coefficients are interrelated via

$$\zeta_{ij} \equiv \frac{RT}{cD_{ij}} \qquad [4]$$

where ζ_{ij} is the frictional coefficient for the interaction between species i and j, defined by assuming that the frictional force $\mathbf{F}_{ij}^*$ (N/mol i) between species i and j, the latter being present in the mixture at unit concentration, is given by, $\mathbf{F}_{ij}^* \equiv -\zeta_{ij}(\boldsymbol{\nu}_i^D - \boldsymbol{\nu}_i^D)$. These, in turn, are related to Spiegler's[28] frictional coefficient f_{ij} by $c_j\zeta_{ij} = f_{ij}$. When applied to diffusional transport within an ion-exchange membrane, itself considered simply as an additional, albeit a large molecular weight "dust" species ($j = M$), within the framework of the dusty-fluid model (DFM),[43] constrained by external clamping forces to be stationary ($\boldsymbol{\nu}_M^D = 0$). Eq. 1 results in

$$\frac{-c_i}{RT}\nabla_T\mu_i^e = \sum_{\substack{j=1\\ j\neq i}}^{n}\frac{c_i c_j}{cD_{ij}^e}(\boldsymbol{\nu}_i^D - \boldsymbol{\nu}_j^D) + \frac{c_i}{D_{iM}^e}\boldsymbol{\nu}_i^D \qquad (i = 1, 2, ..., n) \qquad [5]$$

where the continuum diffusion coefficients D_{ij} have been replaced by their "effective" counterparts, D_{ij}^e, to account for the space-filling aspect and tortuosity of the membrane, the latter reducing the effective driving force gradient. Furthermore, D_{iM}^e, or equivalently ζ_{iM}^e, accounts for the frictional interaction between species i and the matrix, or dust particles. It is to be noted again that each sulfonic acid group along with its associated PTFE backbone is treated as the dust species M, with an EW $\approx$ 1100 for Nafion. The effective and continuum diffusion coefficients are interrelated through[45]

$$D_{ij}^e = K_1 D_{ij} \qquad [6]$$

where K_1 is the DFM structural constant for the molecular diffusion coefficient. Frequently, the relation $K_1 = \epsilon^q$ suffices, where ϵ is the volume fraction of the phase through which the diffusion is occurring. A common value for the so-called Bruggeman exponent, is $q =$

S0013-4651(00)01-112-5 CCC: $7.00

1.5.[31,32] Alternatively, if one adopts the percolation model for this,[15] which includes a percolation threshold ϵ_0 below which the diffusion is improbable owing to the lack of connectivity of the phase through which the diffusion occurs, then

$$K_1 = (\epsilon - \epsilon_0)^q \qquad [7]$$

where the critical exponent q is a universal constant predicted to be about 1.5,[15] although it is frequently used as a fitted parameter.[37] The threshold value ϵ_0 is best determined from experiments as a fitted parameter. This model, with $q = 1.5$, is adopted here in view of the well-known percolation behavior of conductivity in proton-exchange membranes.[15]

The effective membrane diffusion coefficient may similarly be written as

$$D^e_{iM} = K_0 D_{iM} \qquad [8]$$

where K_0 is the DFM constant for the matrix diffusion coefficient. Unlike for K_1, however, no general relationship is available to relate K_0 to the structural properties of the membrane for the case of liquid-phase diffusion, although, for gaseous diffusion, relations are available for the corresponding effective Knudsen diffusion coefficient in terms of the porosity, tortuosity factor, and the mean pore radius.[45] As a result, there is little choice but to treat it as a fitted parameter here, as is commonly done.[32,33]

The total species velocity, in general, comprises a convective component **v** in addition to the diffusive component, *i.e.*, $\boldsymbol{\nu}_i = \boldsymbol{\nu}_i^D + \boldsymbol{\nu}$. The convective velocity resulting from a pressure gradient and/or potential gradient may be given by Schlögl's equation[23]

$$\nu = -\frac{B_0}{\eta}\left[\nabla p + \left(\sum_{j=1}^{n} c_j z_j\right) F \nabla \Phi\right] \qquad [9]$$

where the term in the parenthesis accounts for all charged species in the liquid phase, which for the case of proton transport in fuel cells is only the hydronium ion, but would involve other species for electrolyte transport. Implicit in Eq. 9 is the assumption of radial uniformity of charged species within the pores. In case radial nonuniformity is accounted for, *e.g.*, in terms of double-layer theory, the effective d'Arcy permeability for pressure-driven flow B_0 and that for electro-osmosis B_Φ would not be the same.[40,46] This difference is ignored here. With Eq. 9 in Eq. 5, DFM takes the following form in terms of the total species fluxes $\mathbf{N}_i \equiv c_i \boldsymbol{\nu}_i$

$$-\frac{c_i}{RT}\nabla_T \mu_i^e = \sum_{\substack{j=1 \\ j\neq i}}^{n} \frac{1}{cD_{ij}^e}(c_j \mathbf{N}_i - c_i \mathbf{N}_j) + \frac{\mathbf{N}_i}{D_{iM}^e} + \frac{c_i B_0}{\eta D_{iM}^e}\left[\nabla p + \left(\sum_{j=1}^{n} c_j z_j\right) F \nabla \Phi\right] \quad (i = 1, 2, ..., n) \qquad [10]$$

When summed over all species, the Stefan-Maxwell terms cancel, resulting in

$$\left[\nabla p + \left(\sum_{j=1}^{n} c_j z_j\right) F \nabla \Phi\right] = -\frac{RT}{W}\sum_{j=1}^{n} \frac{\mathbf{N}_j}{D_{jM}^e} \qquad [11]$$

where the term

$$W \equiv 1 + \frac{B_0 cRT}{\eta}\sum_{h=1}^{n} \frac{x_h}{D_{hM}^e} \qquad [12]$$

An alternate form of Eq. 10 is, thus, obtained by using Eq. 8 to eliminate the convection driving force in the brackets

$$-\frac{c_i}{RT}\nabla_T \mu_i^e = \sum_{\substack{j=1 \\ j\neq i}}^{n} \frac{1}{cD_{ij}^e}(c_j \mathbf{N}_i - c_i \mathbf{N}_j) + \frac{\mathbf{N}_i}{D_{iM}^e} - \frac{c_i B_0 RT}{\eta D_{iM}^e W}\sum_{j=1}^{n} \frac{\mathbf{N}_j}{D_{jM}^e} \quad (i = 1, 2, ..., n) \qquad [13]$$

which may alternately be written in the more compact form

$$-\frac{c_i}{RT}\nabla_T \mu_i^e = \sum_{j=1}^{n} H_{ij}^e \mathbf{N}_j \qquad (i = 1, 2, ..., n) \qquad [14]$$

with the effective frictional coefficients incorporating the convective terms being

$$H_{ij}^e = (\delta_{ij} - 1)\left(\frac{x_i}{D_{ij}^e} + \frac{cRTB_0 x_i}{\eta W D_{iM}^e D_{jM}^e}\right) + \delta_{ij}\left(\frac{1}{D_{iM}^e} + \sum_{\substack{h=1 \\ h\neq i}}^{n} \frac{x_h}{D_{ih}^e} - \frac{cRTB_0 x_i}{\eta W (D_{iM}^e)^2}\right) \qquad [15]$$

where, as usual, the Kronecker delta function

$$\delta_{ij} = \begin{cases} 0 & (j \neq i) \\ 1 & (j = i) \end{cases} \qquad [16]$$

If desired, Eq. 14 may be formally inverted to yield an expression that is explicit in species flux

$$\mathbf{N}_i = -\frac{1}{RT}\sum_{j=1}^{n} \kappa_{ij}^e c_j \nabla_T \mu_j^e \qquad (i = 1, 2, ..., n) \qquad [17]$$

where κ_{ij}^e are the elements of the matrix $[H^e]^{-1}$, with elements of the effective frictional coefficient matrix $[H^e]$ being given by Eq. 15. The current density is then obtained from

$$\mathbf{i} = F\sum_{i=1}^{n} z_i \mathbf{N}_i \qquad [18]$$

Proton transport in ionomeric membranes.—We apply the above general model of transport of charged species i in ionomeric membranes to the case of proton transport. Figure 1 shows the PEM as a dusty fluid, in which the polymer matrix along with the attached acid groups are viewed as dust particles comprising the PEM. It is visualized that an acid group HA (*e.g.*, sulfonic acid groups in Nafion) is tethered to each dust particle, which are distributed in a spatially uniform manner. Thus, the molecular weight of the dust species is equal to the PEM equivalent weight. In the absence of a polar solvent, the protons are firmly attached to the pendant acid groups A^- and, consequently, exhibit extremely low conductivity ($\sigma \approx 10^{-7}$ S/cm). In the presence of a proton acceptor solvent BH (*e.g.*, HOH, CH_3OH, etc.), however, these acid groups are induced to dissociate as shown below

$$HA \leftrightarrows A^- + H^+ \qquad K_{HA} = \frac{a_{A^-} a_{H^+}}{a_{HA}} \qquad [19]$$

$$H^+ + BH \leftrightarrows BH_2^+ \qquad K_{BH_2^+} = \frac{a_{BH} a_{H^+}}{a_{BH_2^+}} \qquad [20]$$

so that the overall reaction representing protonation of the solvent by the pendant acid group HA is

S0013-4651(00)01-112-5 CCC: $7.00

$$HA + BH \leftrightarrows BH_2^+ + A^- \qquad K_A = \frac{K_{HA}}{K_{BH_2^+}} = \frac{a_{BH_2^+} a_{A^-}}{a_{HA} a_{BH}} \quad [21]$$

The solvated proton here is shown to be associated with a single solvent molecule, which is not likely to be true. In fact, the number of associated solvent molecules would likely vary with λ, the number of solvent molecules per acid site. For simplicity, however, the stoichiometry shown above is assumed here. In addition, it is assumed that each acid group gives up a single proton, which is the case for sulfonic acid groups, although there would be other groups, *e.g.*, phosphonic acid, when the acid may donate more than one proton. It is further assumed that it is this protonated solvent species BH_2^+ that serves as the major charge carrier much as in liquid electrolytes. For local thermodynamic equilibrium, the concentration of the proton carrier is

$$c_{BH_2^+} = c_{HA,0}\alpha \quad [22]$$

where $c_{HA,0}$ is the concentration of the pendant acid groups per unit volume of pore solution. The degree of dissociation, α, for an ideal solution is obtained by solving

$$K_{A,C} \equiv \frac{c_{BH_2^+} c_{A^-}}{c_{HA} c_{BH}} = \frac{\alpha^2}{(1-\alpha)(\lambda-\alpha)} \quad [23]$$

where λ is the number of solvent molecules per acid site $= c_{BH,0}/c_{HA,0}$. The solution to Eq. 23 provides

$$\alpha = \frac{(\lambda+1) - \sqrt{(\lambda+1)^2 - 4\lambda(1-1/K_{A,C})}}{2(1-1/K_{A,C})} \quad [24]$$

Thus, the extent of dissociation depends upon $K_{A,C}$, *i.e.*, on the relative proton affinities of A^- and BH, or in other words on the strength of the acid group (K_{HA}) and the nature of the solvent ($K_{BH_2^+}$), as well as solvent uptake, λ. It is shown below that the acid dissociation is not complete, in general, even for superacidic membranes such as Nafion.

Conductivity of proton-exchange membranes.—For the case of a proton-exchange membrane consisting of water as the solvent, denoting water as species 2 and the protonated solvent, *i.e.*, hydronium ion (H_3O^+) as species 1, Eq. 13, or equivalently Eq. 14, for this binary case ($n = 2$) reduces to

$$\mathbf{N}_1 = -\left(\frac{c_1}{RT}\right)\frac{1}{\dfrac{1}{D_{1M}^e} + \dfrac{1+(\nu-1)x_1}{D_{12}^e} - \dfrac{cx_1B_0RT}{\eta W D_{1M}^e}\left(\dfrac{1}{D_{1M}^e} - \dfrac{\nu}{D_{2M}^e}\right)} \cdot(\nabla_T\mu_1 + z_1F\nabla\Phi) \quad [25]$$

where the flux ratio, $\nu \equiv -\mathbf{N}_2/\mathbf{N}_1$, and from Eq. 12

$$W = 1 + \frac{cB_0RT}{\eta}\left(\frac{x_1}{D_{1M}^e} + \frac{1-x_1}{D_{2M}^e}\right) \quad [26]$$

We restrict the following discussion to conductivity measurements in a closed conductivity cell, *i.e.*, the case of equimolar counterdiffusion, so that $\nu = 1$. In the case of a fuel cell, of course, this would not hold, and then either ν would be specified by the fuel-cell-reaction stoichiometry (*e.g.*, $\nu = 3/2$ for two hydronium ions diffusing to the cathode to produce one water molecule plus releasing two water molecules that served as proton carriers) or it may be appropriate to write another flux equation for species 2 (water) in terms of its chemical potential gradient. Due to the similarity in species 2 (water) and 1 (hydronium ion), it is further assumed here that $D_{1M}^e \approx D_{2M}^e$. Actually, this along with equimolar counterdiffusion is tantamount to assuming that there is no convection (Eq. 11). Furthermore, the concentration gradient of hydronium ions (species 1) is zero owing to the assumption of spatial uniformity of the sulfonic acid groups coupled with electroneutrality.[40] This is further assumed to imply lack of a chemical potential gradient for the hydronium ions, although a water concentration gradient can produce a nonuniform proton activity coefficient and hence a nonzero chemical potential gradient. With the above assumptions, Eq. 25 reduces to the particularly simple form

$$\mathbf{N}_1 = -\left(\frac{1}{D_{1M}^e} + \frac{1}{D_{12}^e}\right)^{-1}\frac{F}{RT}c_1z_1\nabla\Phi \quad [27]$$

Furthermore, from the use of this expression in Eq. 18, the current density is

$$\mathbf{i} = -D_{12}^e\left(1 + \frac{D_{12}^e}{D_{1M}^e}\right)^{-1}\frac{F^2}{RT}c_1z_1^2\,\nabla\Phi \equiv -\sigma\nabla\Phi \quad [28]$$

assuming that hydronium ions are the only charge-carrying species. Furthermore, from the definition of conductivity in Eq. 28, $z_1 = +1$, and Eq. 22 for the concentration of the hydronium ions

$$\sigma = \frac{F^2}{RT}D_{12}^e\left(1 + \frac{D_{12}^e}{D_{1M}^e}\right)^{-1}c_{HA,0}\alpha \quad [29]$$

Finally, the use of Eq. 7 and the definition $D_{12}^e/D_{1M}^e = \zeta_{1M}^e/\zeta_{12}^e = (K_1/K_0)(D_{12}/D_{1M}) \equiv \delta$ results in

$$\sigma = \frac{F^2}{RT}(\epsilon - \epsilon_0)^q\left(\frac{D_{12}^e}{1+\delta}\right)c_{HA,0}\alpha \quad [30]$$

Alternatively, in terms of the equivalent conductance of hydronium ions in water, $\lambda_1^0 \equiv F^2|z_1|D_{12}^0/RT$ [31]

$$\sigma = (\epsilon - \epsilon_0)^q\left(\frac{\lambda_1^0}{1+\delta}\right)c_{HA,0}\alpha \quad [31]$$

Strictly, the numerator of Eq. 27 should include $\Gamma \equiv D_{12}/D_{12}^0$, the ratio of the diffusion coefficient of hydronium ion to that at infinite dilution. However, Γ is expected to be only slightly concentration dependent,[31] and is, consequently, assumed to be unity. The equivalent conductivity of hydronium ions, of course, is unusually high, *i.e.*, $\lambda_1^0 = 349.8$ S cm^2/equiv in water at 25°C, or $D_{12}^0 = 9.312 \times 10^{-5}$ cm^2/s,[31] and is explained in terms of the Grotthus diffusion mechanism in addition to the usual en masse diffusion.[47]

Some comments are also in order on the magnitude of δ. In addition to structural effects represented by K_1/K_0, which depends upon ϵ or RH, δ depends upon the ratio D_{12}/D_{1M}, which in turn depends upon the difference in collision frequencies of species 1 and 2 and that of 1 and *M*, as well as the molecular weights of species 2 and *M*.[48] The difference in collision frequencies in turn depends upon the size difference between species 2 and *M*. Thus, the ratio D_{12}/D_{1M} is expected to be >1. On the other hand, the ratio K_1/K_0 would be expected to have an inverse dependence on ϵ or λ, being large at low water loading and decreasing at higher loadings. Thus, δ would be a relatively large number at low water loadings and would decrease as ϵ increases, when a diffusing hydronium ion would encounter a water molecule more frequently than it would encounter the polymer matrix. Unfortunately, it is difficult to be more quantitative at this stage. Thus, δ is treated as a fitted parameter here, with its value depending upon the level of hydration.

Membrane hydration and swelling.—The equivalent weight (EW) of the membrane (grams of dry polymer/moles of acid groups) and the partial molar volume of the membrane are interrelated

$$\bar{V}_M \approx \frac{EW}{\rho_0} \quad [32]$$

where ρ_0 is density of the dry membrane. For Nafion 117, 115, or 112, membranes of interest here, the EW = 1100, and ρ_0 =

S0013-4651(00)01-112-5 CCC: $7.00

2.05 g/cm.[3,37] Thus, $\bar{V}_M$ = 537 cm^3/mol. The other properties of Nafion required for use in Eq. 31 include acid group concentration, defined on the basis of per unit volume of pore solution

$$c_{HA,0} = \frac{1}{\lambda \bar{V}_2} \quad [33]$$

where $\bar{V}_2$ is the partial molar volume of water, roughly 18 cm^3/mol. The volume fraction of water in swollen Nafion corresponding to a water loading λ is

$$\epsilon = \frac{\lambda}{\frac{\bar{V}_M}{\bar{V}_2} + \lambda} \quad [34]$$

In addition, a relationship is needed for correlating the water uptake to RH. Recently, Futerko and Hsing[49] utilized a modified version of the Flory-Huggins model for this. Springer *et al.*[38] and Hinatsu *et al.*,[50] on the other hand, simply used a third order polynomial to fit λ *vs.* water-vapor activity, a_2. We find, however, that the water sorption characteristics of Nafion can be well-modeled by an n_2 layer Brunauer-Emmett-Teller (BET) equation[51] with physically meaningful parameters, which is hence adopted here

$$\frac{\lambda}{\lambda_m} = \frac{[Ca_2/(1-a_2)][1-(n_2+1)a_2^{n_2} + n_2 a_2^{n_2+1}]}{1+(C-1)a_2 - Ca_2^{n_2+1}} \quad [35]$$

where the RH or the water vapor activity, $a_2 = p_2/p_2^o$, λ_m is the water loading at monolayer coverage, and n_2 is the total number of water layers in the pores at saturation, which is roughly equal to the maximum number of water molecules per sulfonate divided by λ_m, *i.e.*, $n_2 \approx \lambda_{sat}/\lambda_m$ for a parallel-plate pore geometry.

Results and Discussion

Water uptake by Nafion.—The conductivity of Nafion and other proton-exchange membranes is highly dependent upon their water content, the highest conductivity, σ_{sat}, corresponding to water-equilibrated membranes, which have the highest water uptake, λ_{sat}, for a given imbibition temperature and membrane pretreatment procedure.[50] It is useful to recall that three different Nafion pretreatment protocols have been described in the literature:[52] (*i*) boiling the membrane in water, which results in the so-called E (expanded) form; (*ii*) drying at 80°C, which produces N (normal) form; and (*iii*) drying at 105°C, which produces the S (shrunken) form. Hinatsu *et al.*[50] report that the E form of Nafion 117 absorbs more water (λ_{sat}^{liq} = 23 at 25°C) than the N or S forms, which absorb λ_{sat}^{liq} = 13.5 and 11, respectively, at 25°C. However, this increases with the temperature of immersion, except for the E form membranes, for which it remains independent of temperature. Drying of the membranes at elevated temperatures apparently results in pore shrinkage, which can be reversed only by exposure to water at elevated temperatures.

Curiously, the water uptake in membranes equilibrated with saturated water vapor at otherwise identical conditions is significantly lower than in those immersed in water. Thus, Zawodzinski *et al.*[53] observed that at 30ºC the water content of Nafion 117 equilibrated with liquid water, $\lambda_{sat}^{liq} \approx 22$, while for membrane equilibrated with saturated water vapor, $\lambda_{sat}^{liq} \approx 14$. Further, when a liquid-water equilibrated membrane was removed and suspended over saturated water vapor, λ_{sat} dropped from 22 to 14, indicating that the two states are thermodynamically stable. This phenomenon, sometimes known as Schroeder's paradox, is apparently not uncommon in polymer systems, and is discussed briefly in Ref. 53.

Figure 2 shows the equilibrium sorption from water vapor on Nafion 117 as a function of water vapor activity, or RH, taken from the experimental data of Zawodzinski *et al.*[52] at 30°C as well as those of Morris and Sun[37] at 25°C. These data are also similar to those reported by Pushpa *et al.*,[54] although the data of Hinatsu *et al.*[50] at the higher temperature of 80°C are somewhat different. Although there is some scatter in Fig. 2, it can be seen that Eq. 35 represents the data well with physically realistic values of parameters (λ_m = 1.8, n_2 = 13.5, C = 150) as listed in Table I. The monolayer coverage λ_m was estimated from knowledge of the specific pore surface area S and by using

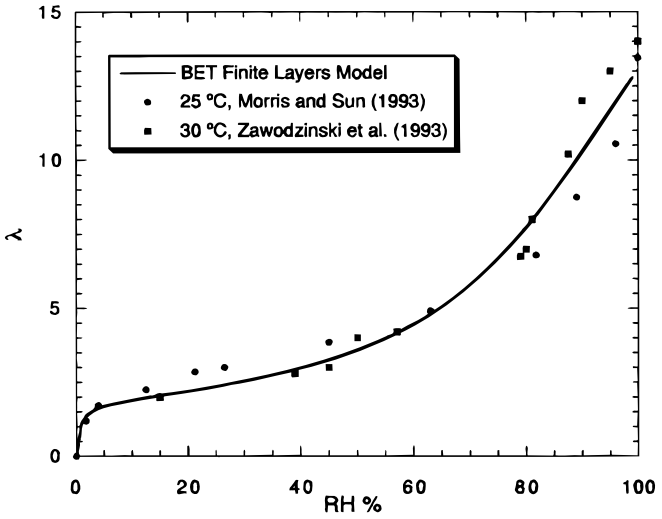

Figure 2. Adsorption isotherm for water uptake by Nafion 117 from water vapor. The finite-layer BET isotherm is compared with the data of Zawodzinski *et al.*[53] at 30°C and that of Morris and Sun[37] at 25°C for the parameters listed in Table I.

$$\lambda_m = \frac{S}{\rho_0}\frac{EW}{N_A A_2} \quad [36]$$

where the surface area occupied by an adsorbate molecule on the pore surface was estimated from[55]

$$A_2 = 1.091\left(\frac{MW_2}{\rho_2 N_A}\right)^{\frac{2}{3}} \quad [37]$$

For Nafion 117, S = 210 (m^2/cm^3),[56] and these expressions provide λ_m = 1.8, which was adopted here. However, as indicated in Table I, C and n_2 were used simply as fitted parameters, but their resulting

Table I. Parameter values employed in model for Nafion membrane.

Parameter	Value	Units	Comments/Reference
EW	1100	g/equiv	Morris and Sun[37]
ρ_0	2.05	g/cm^3	Morris and Sun[37]
S	210	m^2/cm^3	Divisek *et al.*[56]
λ_m	1.8		Calculated from Eq. 36 and S
C	150		Fitted for BET adsorption isotherm, Fig. 2
n_2	13.5		Fitted for BET adsorption isotherm, Fig. 2
λ_0	1.9		Morris and Sun[37]
q	1.5		Gierke and Hsu;[15] Newman[31] p. 461
λ_{sat}^{liq}	23		Hinatsu *et al.*[50]
$K_{A,C,298}$	6.2		Vinik and Zarakhani[61]
ΔH^o	−52.3	kJ/mol	Escoubes and Pineri[57]
E_η	14	kJ/mol	Activation energy for viscosity of water
$\lambda_{1,298}^0$	349.8	S cm^2/equiv.	Newman,[31] p. 255
δ_{sat}^{liq}	0.6		Fitted for liquid-equilibrated conductivity
δ_{sat}^{vap}	5.5		Fitted for vapor-equilibrated conductivity

S0013-4651(00)01-112-5 CCC: $7.00

values are not entirely unreasonable. Thus, $n_2\lambda_m \approx 24$, which is certainly more than $\lambda_{sat}^{vap} \approx 14$, but is of the order of λ_{sat}^{liq}. The parameter C, generally >>1, represents the ratio of the adsorption equilibrium constant of the first layer to that of the subsequent layers

$$C = m \exp\left(\frac{Q_1 - Q_L}{RT}\right) \quad [38]$$

where Q_1 is the enthalpy of adsorption of first layer, while Q_L is that of the succeeding layers, usually assumed to be constant and equal to the latent heat of condensation of the adsorbate. Thus, with $m = 1$, the value of $C = 150$ implies $Q_1 - Q_L \approx 12$ kJ/mol, *i.e.*, at 25°C, $Q_1 \approx 56$ kJ/mol. In comparison, Escoubes and Pineri,[57] based on microcalorimetric studies, found the heat of adsorption of water vapor in Nafion to vary from 16.7 to 52.3 kJ/mol, the higher values corresponding to lower water uptake ($\lambda < 4$). Of course, the assumption of the heat of adsorption of second and higher layers being equal to the heat of condensation (≈ 44 kJ/mol at 25°C for water) may not be true in Nafion due to the strongly hydrophobic nature of the polymer backbone. At any rate, for $Q_1 - Q_L \approx$ constant, Eq. 38 shows that C would decline with temperature, which appears to be consistent with the adsorption isotherms measured at higher temperatures,[50] having a more rounded "knee" at low RHs. Of course, one would also expect n_2 to vary with temperature and the membrane-pretreatment procedure. It appears, in short, that the finite-layers BET adsorption isotherm, with C and n_2 dependent upon temperature and pretreatment procedure, is a suitable representation of adsorption on Nafion.

Finally, it is noteworthy from Fig. 2 that there is a relatively small change in λ over a rather broad range of RH, *i.e.*, from about 10 to 70%. At higher RH, however, the increase in λ is more pronounced, particularly as saturation is approached. This has important implications in the range of RHs required for effective conduction and fuel cell performance, where it is found that there is a precipitous decline in performance at RH substantially less than 100%. This point is further discussed later on.

Conductivity in liquid water-equilibrated membrane.—Since the water content of the membranes immersed in liquid water is quite different from that in those equilibrated with saturated water vapor, the conductivities observed in the two different cases are also significantly different.[53] Therefore, the conductivity of liquid-water equilibrated Nafion®115 was determined experimentally using the alternating curent (AC) impedance method over the temperature range from 25 to 100°C. The conductivity in the longitudinal (*XY*) plane was measured using a pair of pressure-attached, high-surface platinum electrodes. The mounted sample was immersed in deionized and distilled water at a given temperature and equilibrated for 30 min. The conductivity measurements were made with a perturbation voltage of 10 mV in the frequency range from 0.01 to 2.0×10^7 Hz using a Solartron SI 1260 frequency response analyzer. Both real and imaginary components of the impedance were measured, and the real Z axis intercept was closely approximated. The cell constant was calculated from the spacing of the electrodes and the membrane cross-sectional area, *i.e.*, the thickness and the width of the membrane. The experimental results of σ *vs.* inverse temperature are shown in Fig. 3 along with theoretical predictions for the parameters listed in Table I.

The agreement between theory and experiments in Fig. 3 is seen to be good, particularly in view of the fact that $\delta_{sat}^{liq} = 0.6$ was the only fitted parameter employed, all other parameters being adopted from the literature (Table I) and BET constants determined independently as described above. Thus, $\lambda_{sat}^{liq} = 23$ is reported by Hinatsu *et al.*,[50] $\lambda_0 = 1.9$ is given by Morris and Sun[37] (which is also physically realistic in view of $\lambda_m = 1.8$ calculated above), $q = 1.5$ is given by Gierke and Hsu,[15] as well as by Newman,[31] and others,[32] although Morris and Sun[37] propose $q = 1.9$.

The temperature dependence of equivalent conductance is assumed to be given by

$$\lambda_i^0 = \lambda_{i,298}^0 \exp\left[-\frac{E_\eta}{R}\left(\frac{1}{T} - \frac{1}{298}\right)\right] \quad [39]$$

which results from $\lambda_i^0\eta \approx$ constant and the Arrhenius temperature dependence of viscosity. Consequently, $E_\eta \approx 14$ kJ/mol, the activation energy for viscosity of water in the temperature range of interest, is assumed here, along with $\lambda_{1,298}^0 = 349.8$ S cm^2/equiv for protons in aqueous solvents.[31] This value of activation energy adopted is justified in view of the following, even though there is a large variation in activation energies for σ reported in the literature, *i.e.*, from 2 to 16 kJ/mol.[4,35,52] For ordinary liquid-phase diffusion, the relation $\lambda_i^0\eta \approx$ constant stems directly from the well-known relation $D_i\eta/T \approx$ constant,[31] along with the relation between equivalent conductance and diffusivity, $\lambda_i^0 \equiv F^2|z_i|D_i^0/RT$. However, it is well known that for the case of hydronium ions, ordinary diffusion is supplemented with Grotthus hopping.[47] It turns out, nonetheless, that the activation energy for Grotthus conduction is also of the same order (14 to 40 kJ/mol),[35] so that $E_\eta = 14$ kJ/mol seems to be a reasonable estimate.

As shown below, however, the temperature dependence of conductivity is also affected by the degree of acid-group dissociation, α, which varies with temperature owing to the temperature dependence of the acid dissociation constant

$$K_{A,C} = K_{A,C,298} \exp\left[-\frac{\Delta H^o}{R}\left(\frac{1}{T} - \frac{1}{298}\right)\right] \quad [40]$$

which is based on the assumption that the heat of solvation, $\Delta H^o \approx$ constant. Unfortunately, however, the $K_{A,C,298}$ value for Nafion is not available in the literature, although the study of Twardowski *et al.*[58] indicates a pKa < 1, suggesting strong acidity. Furthermore, the Hammett acidity function of Nafion is reportedly similar to that for 100% sulfuric acid.[59] Consequently, it was decided to use the thermodynamics of the liquid solvation reaction

$$H_2SO_4 + H_2O \rightleftarrows H_3O^+ HSO_4^- \quad [41]$$

to simulate that of the sulfonic acid groups in Nafion. For H_2SO_4, the reported $K_{A,C,298}$ values range from 1.2 to 50.[60] Based on the data of Vinik and Zarakhani,[61] $K_{A,C,298} = 6.2$ was adopted for Nafion. It may also be recalled that the study of Escoubes and Pineri[57] found the heat of adsorption of water vapor in Nafion to be 52.3 kJ/mol at $\lambda < 4$. Consequently, $\Delta H^o = -52.3$ kJ/mol in Eq. 40 was adopted. With the above parameters thus chosen from the literature, a choice of $\delta = 0.6$ provides a good fit between the theoretical model and the

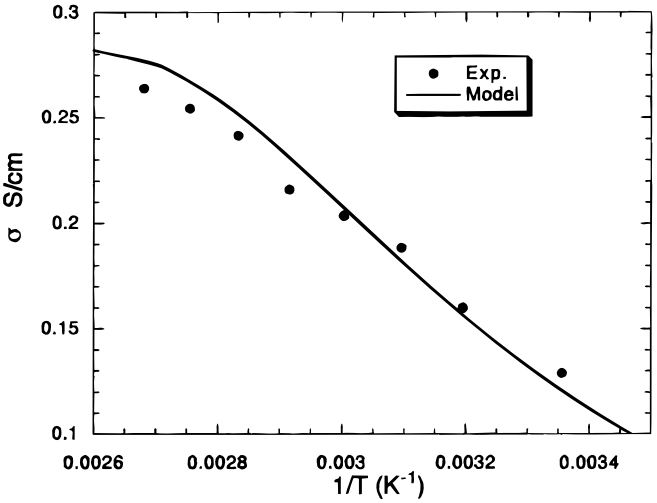

Figure 3. Experimental σ_{max} for Nafion 115 immersed in liquid water *vs.* inverse temperature along with theoretical predictions for parameters listed in Table I.

S0013-4651(00)01-112-5 CCC: $7.00

experimental data as shown in Fig. 3. Particularly noteworthy is the observance that the model captures the decrease in slope, or the effective activation energy, at higher temperatures. This is due to incomplete acid dissociation at the higher temperatures, as discussed below, and may account for some of the discrepancy in activation energies reported in the literature. Interestingly, as a result of this, the theoretical model predicts a maximum in conductivity at higher temperatures, which needs to be confirmed experimentally.

It is of interest to investigate, assuming of course that the acid dissociation constant adopted above is reasonable, whether the sulfonic acid groups are completely dissociated, as is usually assumed, under different conditions of water uptake and temperature. Thus, using Eq. 40 in 24, the degree of dissociation is plotted in Fig. 4 *vs.* λ at different temperatures. It is noteworthy that, even at low temperatures, the dissociation is not complete for $\lambda < 10$. Furthermore, as expected for an exothermic reaction, the dissociation at higher temperatures typical of PEM fuel cells is incomplete even under saturation conditions. Thus, at higher temperatures, higher water contents are required for adequate dissociation. These considerations are clearly of practical significance in view of current efforts to develop higher temperature proton-exchange membranes.[62]

Conductivity in water vapor-equilibrated Nafion.—A predictive model for the dramatic effect of RH on the conductivity of Nafion is, of course, crucial in studying and optimizing fuel-cell performance. Figure 5 compares the model developed here with the data of Sone *et al.*[35] for conductivity of Nafion 117 *vs.* RH for water-vapor-equilibrated membrane at three different temperatures. The agreement is seen to be very good over two orders of magnitude, providing confidence in the soundness of the theoretical approach. Furthermore, the model predicts the effect of temperature on σ adequately in this range. It is noteworthy that the parameter values determined as described above and listed in Table I remain unchanged, except for δ, which takes on a value of 5.5 for water-vapor-equilibrated Nafion. It may be recalled from the discussion that this parameter would be expected to increase as the water content of the membrane declines. It turns out, however, that a single value of $\delta = 5.5$ is adequate for fitting the data over the entire range of RHs. As expected, its value is greater than that for the case of liquid-water-equilibrated membrane. Although it is not yet possible to determine if this value of δ is reasonable, it compares well with the value of $\delta = 3.7$ for the case of Na^+ cation transport through the membrane, used by van der Stegen[33] as a fitted parameter. Finally, it is clear from this figure that RH has a very pronounced effect on the membrane conductivity, explaining the precipitous drop in fuel-cell performance at lower RHs.[62]

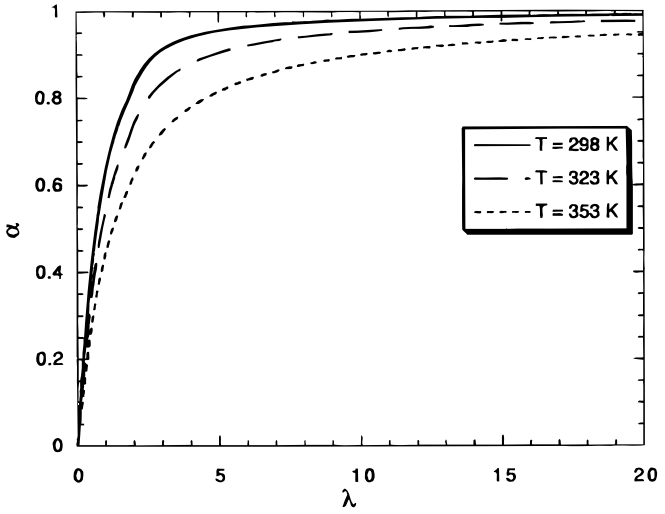

Figure 4. Predicted equilibrium fractional dissociation of sulfonic acid groups in Nafion as a function of the water uptake at different temperatures.

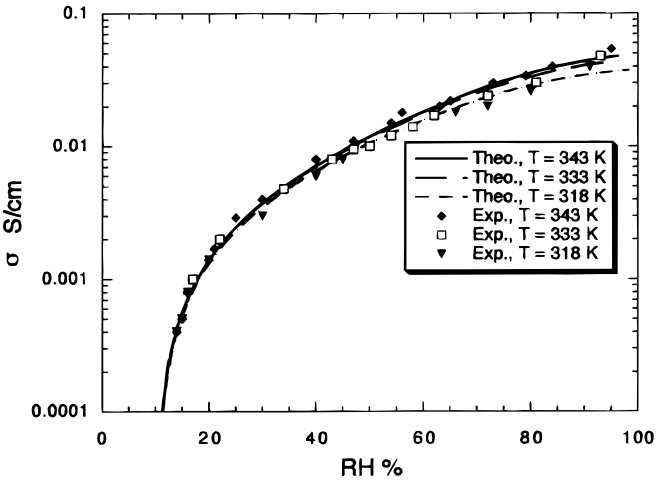

Figure 5. The experimental results of Sone *et al.*[35] for σ of Nafion 117 equilibrated in water vapor *vs.* RH or water vapor activity at different temperatures along with theoretical predictions for parameters listed in Table I.

Effect of temperature on conductivity of vapor-equilibrated Nafion.—The conductivity of Nafion is strongly dependent upon temperature for a given partial pressure of water. This aspect is important due to the current efforts to develop higher-temperature ($\geq$120°C) PEM fuel cells that operate at or around ambient pressure,[62] which would clearly require membranes that perform adequately at lower RHs. Such is not the case, of course, for conventional PFSAs such as Nafion. Thus, Fig. 6 shows the data of Sumner *et al.*[34] for the conductivity of Nafion 117 as a function of temperature at a fixed partial pressure of water (2.0×10^4 Pa, *i.e.*, a humidifier temperature of 60°C) along with the model predictions based on the parameters listed in Table I, with no additional fitted parameters employed. It may be gleaned from this figure that if the temperature of a fuel cell operating at 60°C were raised, for instance, to around 100°C, with the humidifier temperature remaining at 60°C, its performance would drop hopelessly, corresponding to a decline in membrane conductivity of about two orders of magnitude. Malhotra and Datta[62] found this indeed to be the case, which is a major impediment in the development of higher-temperature ambient-pressure fuel cells based on conventional PEMs.

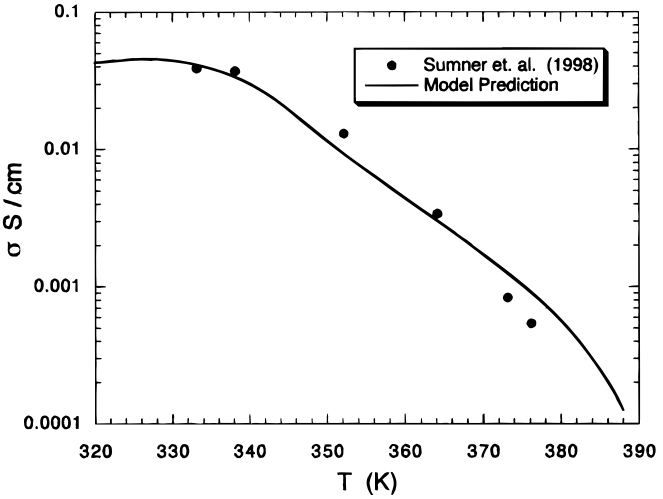

Figure 6. Effect of temperature on conductivity of Nafion 117 at a fixed partial pressure of water (2.0×10^4 Pa, *i.e.*, humidifier temperature = 333 K). The data of Sumner *et al.*[34] are plotted along with model predictions for parameters listed in Table I.

S0013-4651(00)01-112-5 CCC: $7.00

Conclusions

A predictive transport model is proposed here for the conductivity of proton-exchange membranes based on the dusty-fluid model founded on the generalized Stefan-Maxwell equations and including diffusion and convection, the latter resulting from a pressure and/or potential gradients. The theoretical model also incorporates thermodynamic equilibrium analysis for dissociation of the pendant acid groups in the presence of polar solvent such as water. The physicochemical characteristics of the membrane are also included, as is a finite-layers BET model for the sorption isotherm of the solvent by the membrane from the vapor phase. The result is a robust model that is able to provide reliable predictions for the membrane conductivity under a variety of conditions of relative humidity and temperature, as well as for water-equilibrated membranes. All the parameters employed in the calculations were obtained from the literature, with only the BET parameters C and n_2, as well as δ, the ratio of diffusion coefficients representing interaction of the hydronium ion with water and that with the membrane, employed as fitted parameters. These fitted parameters have values that appear justifiable. The described model should be useful in predicting and optimizing the performance of PEM fuel cells.

Acknowledgment

The financial support for this work provided by the H Power Corporation under Naval Surface Warfare Center (NSWC) contract no. N00167-99-C-0002 is gratefully acknowledged.

Worcester Polytechnic Institute assisted in meeting the publication costs of this article.

List of Symbols

a_i	activity of species i
a_2	activity, or relative humidity RH, of water, $= p_2/p_2^o$
A_2	surface area occupied by adsorbate molecule, nm^2
BH	proton acceptor solvent (*e.g.*, HOH)
B_0	d'Arcy permeability, cm^2
c	total concentration of liquid mixture, mol/cm^3 pore solution
$c_{HA,0}$	concentration of membrane acid groups, $= 1/\lambda \bar{V}_2$, mol/cm^3 pore solution
c_i	concentration of species i, mol/cm^3 pore solution
C	BET constant
D_{ij}	mutual diffusion coefficient for species i and j, cm^2/s
D_{ij}^0	mutual diffusion coefficient of species i and j at infinite dilution, cm^2/s
D_{iM}	diffusion coefficient for interaction of species i and matrix M, cm^2/s
D_{ij}^e	effective mutual diffusion coefficient of species i and j within membrane, $= K_1 D_{ij}$, cm^2/s
D_{iM}^e	effective diffusion coefficient for interaction of species i and matrix M, $= K_0 D_{iM}$, cm^2/s
EW	membrane equivalent weight, gram of dry polymer/mole of $-SO_3H$ groups
E_η	activation energy for viscosity, kJ/mol
F	Faraday's constant, 96,487 C/equiv
HA	acid group (*e.g.*, $-SO_3H$) in membrane
$[H^e]$	matrix with elements H_{ij}^e
H_{ij}^e	effective frictional coefficient defined by Eq. 15, s/cm^2
$\mathbf{i}$	current density, A/cm^2
i, j	species i, j
K_0	dusty-fluid model structural constant for matrix diffusion coefficient
K_1	dusty-fluid model structural constant for mutual diffusion coefficient
K_{HA}	equilibrium constant for acid dissociation
$K_{BH_2^+}$	equilibrium constant for solvent protonation
K_A	equilibrium constant for proton solvation, $= K_{HA}/K_{BH_2^+}$
$K_{A,C}$	equilibrium constant for proton solvation in terms of concentrations
n	total number of liquid-phase species
n_2	total number of water layers sorbed on the pore surface
N_A	Avogadro's number, 6.02205×10^{23} molecules/mol
$\mathbf{N}_i$	flux of species i, mol/cm^2 s
p	pressure, N/cm^2
p_i	partial pressure of species i, N/cm^2
p_i^o	vapor pressure of species i, N/cm^2
q	Bruggeman or critical exponent
Q_1	heat of adsorption of first layer, J/mol
Q_L	heat of adsorption of subsequent layers, J/mol
R	universal gas constant, 8.3143 J/mol K
S	specific pore surface area, m^2/cm^3
T	absolute temperature, K
T_0	reference temperature, K
$\boldsymbol{\nu}$	mass-average convective velocity of fluid, cm/s
$\boldsymbol{\nu}_i$	absolute velocity of species i, cm/s
$\boldsymbol{\nu}_i^D$	diffusional velocity of species i with respect to the mixture mass-average velocity, cm/s
$\bar{V}_i$	partial molar volume of species i, cm^3/mol
x_i	mole fraction of species i
z_i	charge number of species i

Greek

α	degree of acid-group dissociation
κ_{ij}^e	elements of inverse matrix $[H^e]^{-1}$, cm^2/s
γ_i	activity coefficient of species i
Γ	ratio of the diffusion coefficient to that at infinite dilution, $= D_{12}/D_{12}^0$
δ	ratio of mutual to matrix effective diffusion coefficients, D_{12}^e/D_{1M}^e
δ_{ij}	Kronecker delta function
ΔH^o	enthalpy change for proton solvation, kJ/mol
ϵ	volume fraction of water in hydrated membrane, or wet porosity
ϵ_0	percolation threshold volume fraction of water in hydrated membrane
ζ_{ij}	friction coefficient for interaction between species i and j, (J s/cm^5)(cm^3/mol)^2
ζ_{iM}	friction coefficient for interaction between species i and matrix M, (J s/cm^5)(cm^3/mol)^2
η	fluid mixture viscosity, g/cm s
λ	water loading, number of water molecules per $-SO_3H$ group
λ_m	water loading at monolayer coverage, number of water molecules per $-SO_3H$ group
λ_0	water loading at percolation threshold, number of water molecules per $-SO_3H$ group
λ_{sat}^{liq}	water loading at saturation in equilibrium with liquid water, number of water molecules per $-SO_3H$ group
λ_{sat}^{vap}	water loading at saturation in equilibrium with saturated water vapor, number of water molecules per $-SO_3H$ group
λ_i^0	equivalent conductance for ionic species i at infinite dilution, S cm^2/equiv
μ_i	chemical potential of species i, J/mol
μ_i^e	electrochemical potential of species i, J/mol
ν	flux ratio, $= -\mathbf{N}_2/\mathbf{N}_1$
ρ	density, g/cm^3
ρ_0	density of dry membrane, g/cm^3
σ	effective conductivity of membrane, S/cm
σ_{max}	maximum effective conductivity of membrane in liquid-equilibrated membrane, S/cm
Φ	electric potential, V

Subscripts

i, j	species i, j
1	H_3O^+
2	H_2O
M	membrane
sat	saturated
T	at constant temperature T
298	at reference temperature, 298 K
0	dry membrane, reference, percolation threshold

Superscripts

e	effective, electrochemical
liq	equilibrated with liquid
o	standard state
vap	equilibrated with vapor
0	infinite dilution

Abbreviations

BET	Brunauer-Emmett-Teller
DFM	dusty-fluid model
EW	equivalent weight, grams of dry polymer/moles of acid groups
GSM	generalized Stefan-Maxwell equations
PEM	proton-exchange membrane
PFSA	polyperfluorosulfonic acid
RH	relative humidity

References

1. W. Grot, in *Encyclopedia of Polymer Science and Engineering*, Vol. 6, 2nd. ed., John Wiley (1989).
2. T. D. Gierke, G. E. Munn, and F. C. Wilson, *J. Polym. Sci., Polym. Phys. Ed.*, **19**, 1687 (1981).
3. S. W. Yeo and A. Eisenberg, *J. Appl. Poly. Sci.*, **21**, 875 (1977).

S0013-4651(00)01-112-5 CCC: $7.00

4. J. Halim, F. N. Buchi, O. Haas, M. Stamm, and G. G. Scherer, *Electrochim. Acta*, **39**, 8/9 (1994).
5. B. Rodmacq, J. M. D. Coey, M. Escoubes, E. Roche, R. Duplessix, A. Eisenberg, and M. Pineri, in *Water in Polymers*, S. P. Rowland, Editor, Chap. 29, ACS Symposium Series **127**, ACS, Washington, DC (1980).
6. H. L. Yeager and A. Steck, *J Electrochem Soc.*, **128**, 1880 (1981).
7. K. A. Mauritz, C. J. Hora, and A. J. Hopfinger, in *Ions in Polymers*, A. Eisenberg, Editor, Chap. 8, Advanced Chemistry Series **187**, ACS, Washington, DC (1980).
8. S. R. Lowry and K. A. Mauritz, *J. Am. Chem. Soc.*, **102**, 4665 (1980).
9. T. D. Gierke, *J Electrochem. Soc.*, **124**, 319(C) (1977).
10. W. Y. Hsu, J. R. Barley, and P. Meakin, *Macromolecules*, **13**, 198 (1980).
11. V. K. Dayte, P. L. Taylor, and A. J. Hopfinger, *Macromolecules*, **17**, 1704 (1984).
12. K. A. Mauritz and C. E. Rogers, *Macromolecules*, **18**, 483 (1985).
13. P. Aldebert, B. Dreyfus, G. Gebel, N. Nakamura, M. Pineri, and F. Volino, *J. Phys. France*, **49**, 2101 (1988).
14. M. Falk, *Can. J. Chem.*, **58**, 1495 (1980).
15. T. D. Gierke and W. Y. Hsu, in *Perfluorinated Ionomer Membrane*, A. Eisenberg and H. L. Yeager, Editors, ACS, Washington, DC (1982).
16. W. Y. Hsu and T. D. Gierke, *Macromolecules*, **15**, 101 (1982).
17. F. Helfferich, *Ion Exchange*, McGraw-Hill, New York (1960).
18. N. Lakshminarayanaiah, *Transport Phenomena in Membranes*, Academic Press, New York (1969).
19. E. Riande, in *Physics of Electrolytes*, Vol. 1, J. Hladik, Editor, p. 401, Academic Press, New York (1972).
20. P. Meares, J. F. Thain, and D. G. Dawson, in *Membranes. A Series of Advances*, G. Eisenman, Editor, p. 55, Marcel Dekker, New York (1972).
21. O. Kedem and A. Katchalsky, *Trans. Faraday Soc.*, **59**, 1918 (1963).
22. A. Katchalsky and P. F. Curran, *Nonequilibrium Thermodynamics in Biophysics*, Harvard University Press, Cambridge, MA (1965).
23. M. Verbrugge and R. Hill, *J. Electrochem. Soc.*, **137**, 886 (1990).
24. E. H. Cwirko and R. G. Carbonell, *J. Membr. Sci.*, **67**, 227 (1992).
25. M. A. Scattergood and E. N. Lightfoot, *Trans. Faraday Soc.*, **64**, 1135 (1968).
26. E. N. Lightfoot, *Transport Phenomena and Living Systems*, Wiley, New York (1974).
27. P. N. Pintauro and D. N. Bennion, *Ind. Eng. Chem., Fundam.*, **23**, 230 (1984).
28. K. S. Spiegler, *Trans. Faraday Soc.*, **54**, 1408 (1958).
29. A. G. Guzmán-Garcia, P. N. Pintauro, M. W. Verbrugge, and R. Hill, *AIChE J.*, **36**, 1061 (1990).
30. P. Pintauro and Y. Yang, in *Tutorials In Electrochemical Engineering-Mathematical Modeling*, R. F. Savinell, J. M. Fenton, A. West, S. L. Scanlon, and J. Weidner, Editors, PV 99-14, p. 178 The Electrochemical Society Proceeding Series, Pennington, NJ (1999).
31. J. S. Newman, *Electrochemical Systems*, 2nd ed., pp. 255, 299, 461, Prentice Hall, Englewoods Cliffs, NJ (1991).
32. J. A. Wesseling, P. Vonk, and G. Kraaijeveld, *Chem. Eng. J.*, **57**, 75 (1995).
33. J. H. G. van der Stegen, A. J. van der Veen, H. Weerdenburg, J. A. Hogendoorn, and G. F. Versteeg, *Chem. Eng. Sci.*, **54**, 2501 (1999).
34. J. J. Sumner, S. E. Creager, J. J. Ma, and D. D. DesMarteau, *J. Electrochem. Soc.*, **145**, 107 (1998).
35. Y. Sone, P. Ekdunge, and D. Simonsson, *J. Electrochem. Soc.*, **143**, 1254 (1996).
36. C. S. Fadley and R. A. Wallace, *J. Electrochem. Soc.*, **115**, 1264 (1968).
37. D. Morris and X. Sun, *J. Appl. Polym. Sci.*, **50**, 1445 (1993).
38. T. E. Springer, T. A. Zawodzinski, and S. Gottesfeld, *J. Electrochem. Soc.*, **136**, 2334 (1991).
39. M. Eikerling, A. A. Kornyshev, and U. Stimming, *J. Phys. Chem. B*, **101**, 10807 (1997).
40. D. M. Bernardi and M. W. Verbrugge, *AIChE J.*, **37**, 1151 (1991).
41. S. J. Paddison, R. Paul, and T. A. Zawodzinski, Jr., *J. Electrochem. Soc.*, **147**, 617 (2000).
42. X.-D. Din and E. E. Michaelides, *AIChE J.*, **44**, 35 (1998).
43. E. A. Mason and A. P. Malinauskas, *Gas Transport in Porous Media: The Dusty-Gas Model*, p. 142, Elsevier, Amsterdam (1983).
44. A. Eisenberg and J. S. Kim, *Introduction to Ionomers*, Wiley-Interscience, New York (1998).
45. R. Jackson, *Transport in Porous Catalysts*, Elsevier, Amsterdam (1977).
46. R. Datta and V. R. Kotamarthi, *AIChE J.*, **36**, 916 (1990).
47. T. A. Zawodzinski, M. Neeman, L. O. Sillerud, and S. Gottesfeld, *J. Phys. Chem.*, **95**, 6040 (1991).
48. F. A. Williams, *Am. J. Phys.*, **26**, 467 (1958).
49. P. Futerko and I.-M. Hsing, *J. Electrochem. Soc.*, **146**, 2049 (1999).
50. J. T. Hinatsu, M. Mizuhata, and H. Takenaka, *J. Electrochem. Soc.*, **141**, 1493 (1994).
51. A. W. Adamson and A. P. Gast, *Physical Chemistry of Surfaces*, 6th ed., p. 622, Wiley Interscience, New York (1997).
52. R. S. Yeo and H. L. Yeager, in *Modern Aspects of Electrochemistry*, No. 16, B. E. Conway, R. E. White, and J. O'M. Bockris, Editors, p. 437, Plenum Press, New York (1985).
53. T. A. Zawodzinski, C. Derouin, S. Radzinski, R. J. Sherman, V. T. Smith, T. E. Springer, and S. Gottesfeld, *J. Electrochem. Soc.*, **140**, 1041 (1993).
54. K. K. Pushpa, D. Nandan, and R. M. Iyer, *J. Chem. Soc., Faraday Trans. 1*, **84**, 2047 (1988).
55. J. J. F. Scholten, *Stud. Surf. Sci. Catal.*, **79**, 419 (1993).
56. J. Divisek, M. Eikerling, V. Mazin, H. Schmitz, U. Stimming, and Yu. M. Volfkovich, *J. Electrochem. Soc.*, **145**, 2677 (1998).
57. M. Escoubes and M. Pineri, in *Perfluorinated Ionomer Membranes*, A. Eisenberg and H. L. Yeager, Editors. ACS Symposium Series No. 180, p. 9, ACS, Washington, DC (1982).
58. Z. Twardowski, H. L. Yeager, and B. O'Dell, *J. Electrochem. Soc.*, **129**, 328 (1982).
59. M. Misono and T. Okuhara, CHEMTECH, **23** (Nov 1993).
60. M. Liler, *Reaction Mechanisms in Sulfuric Acid*, Academic Press, New York (1971).
61. M. I. Vinnik and N. G. Zarakhani, *Dokl. Akad. Nauk SSSR*, **152**, 1147 (1963).
62. S. Malhotra and R. Datta, *J. Electrochem. Soc.*, **144**, L23-L26, (1997).